CHAPTER 3

MRI T2 WEIGHTED THERANOSTIC NANODEVICES AND CHEMOTHERAPY

Sophie Laurent*,†, Luce Vander Elst*,†, Dimitri Stanicki*
and Robert N. Muller*,†

*Department of General, Organic and Biomedical Chemistry,
NMR and Molecular Imaging Laboratory,
University of Mons, 19 Avenue Maistriau,
7000 Mons, Belgium
†Center for Microscopy and Molecular Imaging (CMMI),
8 Rue Adrienne Boland, 6041 Gosselies, Belgium

This chapter presents and compares the different principal methods to prepare superparamagnetic iron oxide nanoparticles (SPION). An important step for biomedical applications is the stabilization with biocompatible non-toxic coating. Numerous ways are proposed in literature using small charged molecules or polymers. The applications described here are focused on the drug delivery associated to magnetic resonance imaging (MRI) to follow the therapeutic aspect and to control the efficiency of the treatment.

Theranostic devices are defined as systems which combine the modalities of diagnosis and therapy. These materials allow to diagnose by imaging or to follow a real-time medical treatment and to deliver therapeutic drugs in the same time.[1,2]

Among numerous nano-systems, magnetic nanoparticles such as SPION have gained significant attention.[2,3] These SPION present a lot of advantages as (i) their intrinsic magnetic properties for magnetic resonance imaging (MRI),[4] (ii) their lack of toxicity[5] and (iii) their surface coated with biocompatible coatings allowing specific targeting for molecular imaging.[6,7] These properties open large possibilities for biomedical applications: *in vivo* medical imaging, tissue repair, hyperthermia, drug delivery, biosensor, …[8–11] This chapter is focused on the study of SPION as nanocarriers for drug delivery.

One of the most important problems to overcome is the physiological barriers to allow access to cellular target. After intra-venous injection, blood can induce SPION agglomeration or interactions between SPION and plasma proteins, extravascular matrices. Thus, there is a real problem for reaching the target tissues. Another problem is the blood–brain barrier (BBB). Only nanoparticles with sufficiently small size and appropriate physicochemical properties can pass through the BBB. Biodistribution, pharmacokinetics and *in vivo* cellular uptake are directly linked to the physicochemical properties of the SPION (hydrodynamic size, charge surface, shape, coating nature or morphology). For example, hydrodynamic size influences the SPION concentration in the blood vessel[12,13] and affects their clearance from circulation.[14–16] Small nanoparticles (diameter <20 nm) are excreted renally,[14,17] medium sized ones (30–150 nm) are accumulated in the bone marrow, heart, kidney and stomach,[17] while large nanoparticles (150–300 nm) are found in the liver and spleen.[18] A review has suggested that BBB crossing is influenced by several physiochemical properties and not only by the size of the nanoparticles.[19] It has been shown that anisotropically shaped nanoparticles can avoid bio-elimination better than spherical ones.[20]

Charge and hydrophobicity affect biodistribution by interactions of nanoparticles with plasma proteins, immune system, extracellular

matrices or non-targeted cells.[21] Hydrophobic nanoparticles have short circulation times due to adsorption of plasma proteins (opsonization) which can lead to recognition by the reticulo-endothelial system (RES), followed by removal from circulation. Positively charged nanoparticles can also bind with non-targeted cells leading to non-specific internalization. Hydrophobic groups on the surface can induce nanoparticle agglomeration after injection, leading to rapid removal by the RES. To limit these interactions, surface engineering has led to the development of stealth nano-objects. Surface modifications with molecules like the hydrophilic polyethylene glycol (PEG) have been shown to reduce the potential for opsonization through steric repulsion, prolonging NP circulation times.[21]

1. Preparation of Magnetic Nanosystems

SPION can be obtained by top-down (mechanical attrition) or bottom-up (chemical synthesis) approaches. Among these two procedures, chemical routes allow to produce nanoparticles with better control of composition and size.[22] Solution chemical methods include standard iron chloride co-precipitation, thermal decomposition, hydro-thermal synthesis, co-precipitation in constrained environments, sonochemical methods and polyol synthesis. Some reviews on these methods have been reported.[2,4,23] Each method has its own advantages and disadvantages. The most common preparation method involves the mixing of ferric and ferrous derivatives, generally chlorides[24] or sulfates[25] in aqueous solution. The precipitation occurs after the addition of a base (NaOH or NH_4OH) to a solution of ferrous and ferric salts under inert atmosphere at ambient temperature or at high temperature. The main advantage is the ability to produce iron oxide nanoparticles in large quantities. However, the control of the size distribution and of the shape is not efficient. The adjustment of some parameters[23,26–28] such as pH, ratio between Fe (II) and Fe (III) concentrations, ionic strength of medium, salt type, base nature and reaction temperature, allows a better control of the final characteristics of nanoparticles (size, shape and composition). The experimental challenge in the synthesis by co-precipitation is the control

of the particle size to obtain a narrow particle size distribution. As-obtained particles tend to be rather polydisperse. To improve the uniformity and stability of SPION, modifications of the standard co-precipitation approach have been investigated by the use of organic additives as stabilization or reducing agents. Addition of polymers or polyelectrolytes to the iron chloride solution during co-precipitation can tune the physical properties (size, shape and crystallinity) of the SPION.[29,30] These polymers (for example, poly (acrylic acid)[29] or polyethyleneglycol-g-poly(glycerol monoacrylate)[30]) can act as surface coatings after complete nucleation and growth. These coatings are referred to as *in situ* because they are present during nanoparticle synthesis. Unfortunately, this approach can limit the crystallinity of SPION, which may affect their magnetic susceptibility.

More recently, some synthesis techniques have used high-temperature decomposition methods and organic iron precursors.[31,32] Sun *et al.* reported high-temperature reaction of iron (III) acetylacetonate, $Fe(acac)_3$, in phenylether or dibenzylether in the presence of alcohol, oleic acid and oleylamine, to yield monodisperse hydrophobic NPs with tunable sizes of 4–20 nm.[32] This strategy is promoted by the use of the seed-mediated growth method. Nanoparticle size increases up to 20 nm via the addition of new quantity of iron precursor in the nanoparticle suspension without the modification of size standard deviation. Hyeon *et al.*[33] reported the production of monodisperse iron oxide nanoparticles by using thermal decomposition of iron pentacarbonyl ($Fe(CO)_5$) in a solution of octylether containing oleic acid to yield an iron oleate complex at low temperature. Then, the iron oleate solution was decomposed at high temperature (300°C) to obtain 11 nm monodisperse iron nanoparticles followed by a controlled oxidation with trimethylamine as a mild oxidant, in order to form iron oxide nanoparticles.

Park *et al.*[34] also developed a similar approach to produce monodisperse nanoparticles in which the nanoparticle size is increased by one nanometer between each step. They used iron chloride and sodium oleate to generate an iron oleate complex *in situ* which was then decomposed at temperature between 240°C and 320°C in different

solvents, such as 1-hexadecane, octylether, 1-octadecene, 1-eicosene or trioctylamine. Jana *et al.* described a decomposition approach for the synthesis of size and shape controlled magnetic oxide nanocrystals based on the pyrolysis of metal fatty acid salts in non-aqueous solution.[35] The process has exploited a large panel of fatty acids (such as decanoic acid, lauric acid, myristic acid, palmitic acid, oleic acid or stearic acid), hydrocarbon solvents (octadecene, n-eicosane, tetracosane, or a mixture of octadecene and tetracosane) and activation agents (primary amines or alcohol). Nearly monodisperse iron oxide nanoparticles could be produced. This process allows a size control (size range of 3–50 nm) and a shape control (spherical or cubic) according to the variation of concentration and the length of fatty acids. The limitation of these synthesis approaches is that additional steps are required to remove the hydrophobic coating, or to modify the surface with an amphiphilic surfactant to render the nanosystems usable for biomedical applications. A very simple synthesis of water soluble magnetite nanoparticles was reported by Li.[36] Using $FeCl_3 \cdot 6H_2O$ as iron source and 2-pyrrolidone as coordinating solvent, water soluble Fe_3O_4 nanocrystals were prepared under reflux (245°C). The same team developed a one-pot synthesis of water soluble magnetite nanoparticles prepared under similar reaction conditions by the addition of α,ω-dicarbonyl terminated PEG as a surface capping agent.[37] Even if these new techniques yield more uniform nanoparticles with superior magnetic properties, the co-precipitation method continues to be most widely used for biomedical applications because of an easy implementation and less hazardous materials and procedures.

Microemulsion and inverse micelle syntheses have been employed to prepare shape and size controlled SPION. Particularly, water-in-oil (w/o) microemulsions are formed by well-defined nano-droplets of the aqueous phase, dispersed by the assembly of surfactant molecules in a continuous oil phase. Microemulsion cavities can be considered as reactors. Most of the used methods are based on the coprecipitation process of iron precursors in basic condition. Two general methods could be used for the formation of magnetite nanoparticles. The first process is made up of two different microemulsions where the

first one contains the iron precursors and the second one contains the base. By the mixing of both water in oil microemulsion systems, the colloid microdroplets coalesce and finally a precipitate appears in the micelles. The second method is composed of a microemulsion containing the iron precursors in which the base is then added. This induces the beginning of the coprecipitation mechanism. Vidal-Vidal *et al.*[38] have reported the synthesis of monodisperse SPION by a "one pot" microemulsion method. The spherical shaped particles capped with a monolayer coating of oleylamine show a narrow size distribution of 3.5 nm. Okoli *et al.*[39] described a complex microemulsion system based on the mixing of two microemulsion systems. The first microemulsion is obtained by the mixing of iron precursors (iron (II) and (III) chlorides) with the surfactants (CTAB: cetyltrimethylammonium bromide), co-surfactant (butanol), water and oil phase (*n*-octane). The second mixture containing the precipitating agent (NH_3) is slowly added to the first microemulsion where the reaction occurs and produces the formation of iron oxide nanoparticles.

Masih and coworkers[40] proposed an easy microemulsion method where the organic surfactants molecules (igepal-CO 520 (polyoxyethylene-(5)-nonylphenylether)) act both as a stabilizer of the microemulsion and as a capping layer surrounding the final nanoparticles.

In comparison to the nanoparticles produced by Massart team procedure,[41] particles obtained by microemulsion technique were smaller in size and had higher saturation magnetization.[42] Although the work-up of the synthesis is simple and fast, the elimination of surfactant excess requires the use of robust purification methods. Moreover, the total yield of the reaction is quite low as compared to other methods. To produce a large quantity of nanoparticles, it is necessary to use large amounts of solvent and surfactants. Therefore, it is obvious that the scale-up of the process is difficult.

The microemulsion and thermal decomposition methods usually lead to complex process or require relatively high temperature. As an alternative way, hydrothermal synthesis includes various wet-chemical technologies of crystallizing substance in a sealed reactor or autoclave systems at high temperature aqueous solution (130–250°C) and high vapor pressure (0.3–4 MPa). Several authors reported the synthesis of

SPION by hydrothermal method[43–45] with or without the presence of specific surfactants. Wang *et al.*[46] reported a one-step hydrothermal process to prepare highly crystalline Fe_3O_4 particles without surfactant. On the contrary, Zheng *et al.*[47] described a hydrothermal route for preparing Fe_3O_4 nanoparticles with a diameter of about 27 nm in the presence of sodium bis (2-ethylhexyl) sulfosuccinate (AOT) as surfactant.

Ge *et al.*[48] described a hydrothermal synthesis in which the nanoparticles were formed from the oxidation of ferrous chloride in basic aqueous solution (NH_4OH) under a high temperature (134°C) and a high pressure (2 bars). By the variation of experimental parameters such as iron precursor concentration, the particle diameter can be tuned from 15 nm to 31 nm. Although nearly monodisperse iron oxide nanoparticles can be formed, this synthetic strategy needs the use of extreme experimental conditions (high temperature and high pressure).

The sonochemical method has also been used to generate SPION.[49] The chemical effects of ultrasound from acoustic cavitation are the formation, growth and implosive collapse of bubbles in solution. The implosive collapse of the bubble generates a localized hotspot with transient temperatures of 5000 K, pressures of 1,800 atm, and cooling rates in excess of 1,010 K/s.[50] SPION can be simply synthesized by sonication of iron (II) acetate in water under an argon atmosphere. Vijayakumar *et al.*[51] reported a sonochemical synthetic route to prepare SPION with a size of 10 nm. These nanoparticles are superparamagnetic but their magnetization is very low. More recently, Pinkas *et al.*[52] developed a sonochemical synthetic method for preparing amorphous particles by sonolysis of $Fe(acac)_3$ under Ar with a small amount of water. The organic content and the surface area of the SPION can be controlled with an amount of water in the reaction mixture.

During the SPION synthesis, the polyols can be also used as capping agents for the control of particle growth and for the limitation of the agglomeration phenomena. Joseyphus *et al.*[53] studied the polyol influence on nanoparticle formation. Several parameters govern the production of particles such as the type of polyols, the iron (II)

chloride precursor concentration, the hydroxide sodium concentration and reaction temperature. Zhang *et al.*[54] reported a thermolysis of iron (III) acetylacetonate in PEG associated with other polymer as poly(vinylpyrrolidone) (PVP) or poly(ethylene imine) (PEI). The nanoparticle size could be tuned in the range of 4.1–14.9 nm by the variation of experimental factors such as the reaction temperature, the reaction time and the PVP or PEI portions. This work demonstrated that the nanoparticles coated with PEG/PVP or PEG/PEI exhibit a much better stability in aqueous media than the PEG coated-nanoparticles. Bridot *et al.*[55] suggested the synthesis of iron oxide cores by the polyol method, which consists of the precipitation of metal oxide in high boiling point alcohol. Adding solid NaOH to iron chloride salts dissolved in diethyleneglycol (DEG) produces a black precipitate of agglomerated SPION that can be washed and suspended in acidic media as previously described,[56] then the iron oxide nanoparticles are stabilized by triethoxysilanepropyl succinic anhydride (TEPSA). In comparison to other methods, this approach presents several advantages. Indeed, this process allows the formation of non-agglomerated nanoparticles with well-defined shape and size. Due to its high boiling point, the polyol can be used as a solvent as well as a reducing agent and a surfactant. Although the polyol method offers a multitude of advantages, the scale-up does not allow the formation of uniform particles in term of size.

The above cited synthetic methods have some advantages and disadvantages for preparing SPION. In terms of size and morphology control of NP, thermal decomposition and hydrothermal synthetic ways seem the optimal method. To obtain hydrophilic biocompatible SPION, co-precipitation often is employed, but this method shows low control of the particle shape, broad distributions of sizes and some nanoparticle aggregations.

2. Coating and Stabilization of Magnetic Iron Oxide Nanoparticles

After synthesis, unmodified SPION are stable in high and low pH suspensions, but their *in vivo* use needs a specific coating. Surface modification and functionalization play critical roles in the

development of any nanoparticle platform for biomedical applications. These surface coatings, small organic molecules or polymers, have to (i) protect against iron oxide agglomeration, (ii) provide reactive chemical functions for the conjugation of drug molecules or targeting ligands and (iii) limit non-specific cell interactions.

In the literature, the main coating agents are polymers (synthetic or naturals), small organic molecules, silica shell and biological molecules. A common strategy used for the surface modification is the formation of a silica shell. To proceed, alkoxysilane molecules or tetraethyl orthosilicate (TEOS) are generally used.[57] The advantage is that the silane groups can be covalently bound onto nanoparticle surface through the reaction between the hydroxyl groups present on iron oxide surface and the alkoxysilane functions (–Si–O–R where R is commonly methyl or ethyl group).[58] The cross-linking events induce the formation of a silica layer around the particles.[59] A large choice of terminal functional groups (alcohol, amine, epoxy, thiol and carboxylate)[60–62] can be used in order to protect iron oxide nanoparticles.

In the same way, coating agents with precious metal (such as gold) also are an effective protection to avoid the surface oxidation and to reduce nanoparticle agglomeration in aqueous solution.[63,64]

Small organic molecules are frequently used to stabilize the magnetic nanoparticles. The chemical functions used generally are carboxylates, phosphates and sulfates due to their high affinity for iron oxide surface. These strong interactions result from an ionic interaction between the acidic functions of the coating agents and the hydroxyl groups of nanoparticles. The most used carboxylic acids are citric and dimercaptosuccinic acids.[65,66] These polyacids form a stable colloidal suspension resulting from the high coordination on metal surface. Unfortunately, the ionic bonds between the carboxylic functions and the iron oxide surface are labile and can be easily broken by the elevation of temperature or by carboxylic compounds presenting a much higher affinity with the surface. Phosphate and phosphonate derivatives are also promising stabilizing candidates. Their absorption on metal surface is very stable and is able to form a strong interaction in aqueous solution.[67,68] In some works, bisphosphonate compounds were preferred in order to anchor double functions on the metal surface, involving the strengthening of the nanoparticle stability.[69,70]

The stabilization performed by biological molecules is not a common method. Some examples describe the surface covering with proteins such as avidin[71] or human serum albumin (HSA).[72,73] This process allows the formation of stable and biocompatible magnetic fluids.

Polymer coating offers the ability to obtain a biocompatible and biodegradable surface and to improve the blood circulation times depending on the polymer nature.[74,75] These polymers can be natural[76] or synthetic.[74,77]

Thanks to its interesting characteristics such as biocompatibility and biodegradability, one of the most natural polymers is dextran.[78] This polysaccharide can be strongly absorbed on nanoparticle surface, due to a strong interaction with hydrogen bonds formed between the hydroxyl groups present on the polymer chains and the surface of iron oxide cores.[79,80] Several preclinical MRI contrast agents have been elaborated with a dextran coating or its derivatives (carboxydextran and carboxymethyl).[81]

Typically, conventional dextran coatings are based on the cross linking of the polymer after the nanoparticle attachment using epichlohydrin.[82,83] The system has demonstrated a high circulation half-life in blood with no acute toxicity. However, other strategies were developed. Duguet *et al.*[84,85] reported the modification of the dextran structure by silane molecules. This strategy allows the covalent grafting on the surface. Although dextran is the favorite natural polymer, other polymers can be used such as chitosan,[86–88] gelatin,[89] alginate[90] and pullulan[91] as stabilizing agents. Another natural and biodegradable polymer is polylactic acid that can be used for the preparation of stable colloid suspension with typical hydrodynamic diameters ranging between 10 and 180 nm.[92,93]

Among the synthetic polymers, PEG is widely used due its properties such as the improvement of blood circulation time, hydrophilicity and biocompatibility. The process is commonly called PEGylation. It can also be coupled with other polymer to increase the hydrophilic properties. Two approaches are currently used to coat nanoparticles and consist in the addition of surfactants during the synthetic process or post-synthesis. Other polymers and copolymers

which have been used to coat magnetic nanoparticles are polyvinyl alcohol (PVA),[94] polystyrene (PS),[95] PVP,[96] poly(acrylic acid) (PAA),[97] poly(ethylenimine) (PEI),[98–100] PAA-chitosan,[101] PEG,[102,103] dextran,[104] phospholipids.[105]

Polymeric coatings have been engineered to enhance SPION pharmacokinetics and tailored drug loading and release behaviors. Different polymers have been investigated where SPION coating was achieved via several approaches including *in situ* coating, post-synthesis adsorption or post-synthesis grafting. The two first coating methods (*in situ* and post synthesis modifications) with polymers (polysaccharides or copolymers) lead to coatings that uniformly encapsulate cores and in the third one (end grafted polymers), PEG (for example) is anchored to the nanoparticle surface by the polymer end groups, forming brush like extensions. Phospholipids form shell around the SPION core and the structure presents hydrophobic regions which can be used for drug encapsulation and delivery.

3. Drug Delivery Systems

The treatment of malignant tumors is a real challenge. The selective delivery of therapeutic agents into a tumor enhances the antitumor efficacy and decreases toxicity in normal tissues.[106–108] Drug delivery involves an easy concept: a small platform is used to deliver the appropriate amount of drug to a desired location inside the body. Moreover, using this technique allows regulation of the drug amount and of the delivery duration.

Nanoparticle-drug systems can accumulate to higher concentrations in certain solid tumors than free drugs via the enhanced permeability and retention (EPR) effect. In addition, actively tumor-targeted nanoparticles may further increase the local concentration of drug or change the intracellular biodistribution within the tumor via receptor-mediated internalization. For drug delivery systems, two main properties are required: firstly, the drug targeting to the desired region must reduce the side effects and secondly, the controlled release of the drug must avoid the classical overdoses. Numerous systems can be used such as micelles,[109,110] liposomes,[111] polymersomes,[112,113]

nanoparticles,[114,115] dendrimers[116,117] or polymers.[118] All these systems are based on the same principle.

The drug is entrapped, attached, adsorbed, or encapsulated into or onto nano-matrices. Superparamagnetic nanoparticles are considered as an efficient nanovector since after their injection, the hybrid compounds can be transported by blood circulation and be concentrated in the tumor region by applying magnetic field on the specific target sites. Moreover, MRI can be used to validate the localization of magnetic drug delivery systems.

Therapeutic entities, such as small drugs, peptides, proteins or nucleic acids, can be incorporated in the SPION through loading on the surface layer or trapping within the nanoparticles themselves. When delivered to the target site, the loaded drugs are usually released by (i) diffusion, (ii) vehicle rupture or dissolution, (iii) pH-sensitive dissociation. Such delivery carriers have many advantages, including water-soluble, low toxic or non-toxic, biocompatible and biodegradable, long blood retention time and capacity for further modification. These therapeutic nanoparticle conjugations enable the simultaneous estimation of tissue drug levels and monitoring of therapeutic response.[119,120]

The drug is generally coupled on nanoparticle surface by covalent or ionic bonds. To release the drug in these specific sites, the link between the magnetic core and the drug must be cleaved. The link cleavage can be ensured by different external stimuli such as pH modification, temperature change or enzymatic cleavage.

Conventional anti-cancer agents such as doxorubicin (DOX) have been conjugated with tumor-targeted IO nanoparticles to achieve effective delivery. Recently Yang *et al.*[121] described folate receptor (FA) targeted SPION to deliver DOX to tumor cells (Figure 1). SPION were encapsulated in the multifunctional polymer vesicles in aqueous solution, the hydrophilic PEG bearing the FA targeting ligand located in outer layers, while the short hydrophilic PEG bearing the acrylate groups located in inner layers. DOX was conjugated onto the hydrophobic polyglutamate polymer segments via an acid-cleavable hydrazone bond and could be released at low pH value. FA-conjugated SPIO/DOX-loaded vesicles showed higher cellular

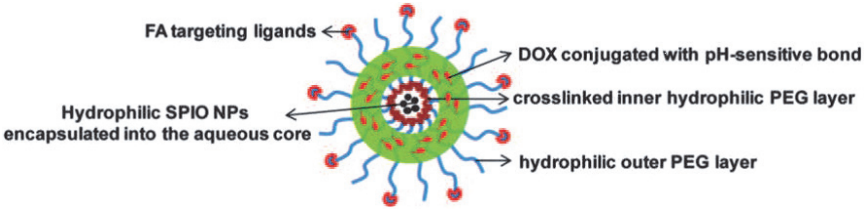

Fig. 1: Scheme of the amphiphilic triblock copolymers and the preparation process of the SPIO/DOX-loaded vesicles with cross-linked inner hydrophilic PEG layers. Reproduced with permission from Ref. 121.

uptake and cytotoxicity compared with FA-free vesicles due to FA-mediated endocytosis.

RNA interference (RNAi) is a promising molecular therapeutic tool due to its high specificity but small interfering RNA (siRNA) cannot reach the target tissue with a sufficient concentration due to RNase degradation. SPION have been used for delivering siRNA and monitoring their efficacy of therapy. Kumar *et al.*[122] synthesized a novel tumor targeted nano-system which consists of peptides (EPPT) that specifically target the antigen uMUC-1, SPION, NIR dye (Cy 5.5) and siRNA that targets the tumor-specific anti-apoptotic gene BIRC5. Systemic delivery to mice bearing human breast adenocarcinoma tumors showed significant increase of R_2 relaxation rate in the tumor, which remained significantly higher than the pre-injection values over time, suggesting that the concentration of nano-drug within the tumor tissue could be maintained. This confirmed and highlighted the feasibility to follow the accumulation and retention of drug-SPION *in vivo* by MRI. The efficacy of this system in the breast tumors was evaluated and showed a five-fold increase in the fraction of apoptotic nuclei in tumors.

Yang *et al.* prepared multifunctional magneto-polymeric nanohybrids (MMPN) modified with antibodies to target breast cancer and followed the treatment by MRI.[123] To obtain these systems, they encapsulated both magnetic hydrophobic nanoparticles and anticancer drug like DOX in an amphiphilic block copolymer. The *in vivo* drug release is observed thanks to the polymer degradation. MRI

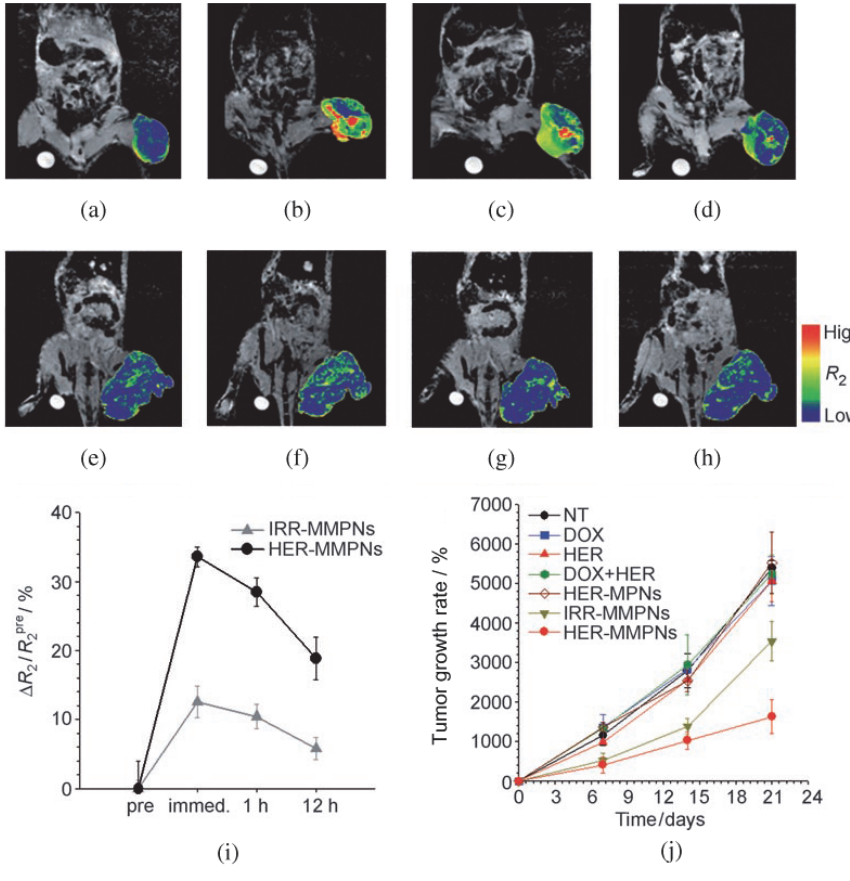

Fig. 2: MR images and color maps of the tumor region of cancer-targeting events of HER–MMPNs (a–d) and IRR–MMPNs (e–h) in NIH3T6.7 cells implanted in mice at various time intervals: (a), (e) pre-injection; (b), (f) immediately; (c), (g) 1 h; (d), (h) 12 h after injection of the MMPNs. (i) DR2/R2 pre-graph vs time before and after injection of MMPNs. (j) Comparative therapeutic-efficacy study in an *in vivo* model. Reproduced with permission from Ref. 123.

studies were performed on mice implanted in their proximal thigh region with NIH3T6.7 cell lines. Two kinds of MMPN were injected as contrast agents: HER–MMPN (nanoparticles conjugated with anti-herceptin antibody) and IRR-MMPN (nanoparticles conjugated with human IgG). The results are shown in Figure 2. HER–MMPN and IRR–MMPN induced tumor growth inhibition as compared with

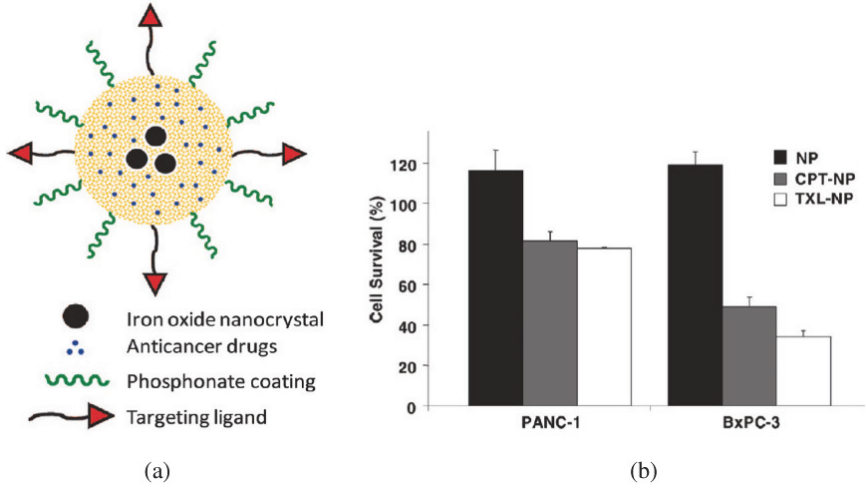

(a) (b)

Fig. 3: Specific multifunctional mesoporous silica with encapsulated iron oxide nanoparticles and anticancer drugs (a); cell growth inhibition results showing therapeutic effect of drug (CPT= camptothecin and TXL= paclitaxel)-loaded nanosystèmes on two different pancreatic cancer cells (PANC-1 and BxPC-3). Drug free control nanoparticles were tested and were non- toxic. Reproduced with permission from Ref. 124.

control group (DOX, HER, DOX + HER or HER – MPN (HER conjugated with a non-drug loaded magnetic nanoparticles)). This article demonstrates the ability to design novel nanodrugs for diagnosis and treatment of different cancers.

Another example of drug delivery and imaging applications has been described by Liong *et al.*[124] The multifunctional nano-platform is based on fluorescent mesoporous silica nanoparticles where superparamagnetic iron oxide nano-objects and anticancer drugs (camptothecin or paclitaxel) are encapsulated (Figure 3). Surface conjugation with folic acid allows to increase the uptake into cells that overexpress FA and thus the drug delivery to cancer cells.

4. Conclusions

SPION are very promising for theranostic agents involving drug delivery and MR imaging. Numerous applications have already been

described in literature and highlight the advantages of combining imaging and therapy (for example, see review in Refs. 125–128).

Acknowledgments

The ARC (research contract AUWB-2010 — 10/15-UMONS-5), the FNRS, ENCITE program, the COST TD1004 (Theranostics imaging and therapy: an action to develop novel nanosized systems for imaging-guided drug delivery), the Walloon Region (first spin-off program), the UIAP VII program and the Center for Microscopy and Molecular Imaging (CMMI, supported by the European Regional Development Fund and the Walloon Region) are thanked for their support.

References

1. V. P. Torchilin, *Adv. Drug Del. Rev.*, 58, 1532 (2006).
2. C. Sun, J. S. H. Lee, M. Q. Zhang, *Adv. Drug Del. Rev.*, 1252 (2008).
3. J. R. McCarthy, R. Weissleder, *Adv. Drug Del. Rev.*, 60, 1241 (2008).
4. S. Laurent, D. Forge, M. Port, A. Roch, C. Robic, L. V. Elst, R. N. Muller, *Chem. Rev.* 2064 (2008).
5. N. Lewinski, V. Colvin, R. Drezek, *Small,* 26 (2008).
6. A. K. Gupta, R. R. Naregalkar, V. D. Vaidya, M. Gupta, *Nanomedicine,* 23 (2007).
7. R. D. K. Misra, *Mater. Sci. Technol.*, 1011 (2008).
8. C. Corot, P. Robert, J. M. Idee, M. Port, *Adv. Drug Del. Rev.,* 1471 (2006).
9. J. D. G. Duran, J. L. Arias, V. Gallardo, A. V. Delgado, *J. Pharm. Sci.,* 2948 (2008).
10. A. Solanki, J. D. Kim, K. B. Lee, *Nanomedicine,* 567 (2008).
11. B. Thiesen, A. Jordan, *Int. J. Hyperthermia,* 467 (2008).
12. P. Decuzzi, M. Ferrari, *Biomater.,* 5307 (2006).
13. P. Decuzzi, F. Causa, M. Ferrari, P. A. Netti, *Ann. Biomed. Eng.,* 633 (2006).
14. H. S. Choi, W. Liu, P. Misra, E. Tanaka, J. P. Zimmer, B. I. Ipe, M. G. Bawendi, J. V. Frangioni, *Nat. Biotech.*, 1165 (2007).

15. W. C. Zamboni, *Oncologist,* 248 (2008).
16. S. M. Moghimi, A. C. Hunter, J. C. Murray, *Pharmacol. Rev.,* 283 (2001).
17. T. Banerjee, S. Mitra, A. K. Singh, R. K. Sharma, A. Maitra, *Int. J. Pharm.,* 93 (2002).
18. S. M. Moghimi, *Adv. Drug Del. Rev.,* 103 (1995).
19. Y. E. L. Koo, G. R. Reddy, M. Bhojani, R. Schneider, M. A. Philbert, A. Rehemtulla, B. D. Ross, R. Kopelman, *Adv. Drug Del. Rev.,* 1556 (2006).
20. Z. Liu, W. B. Cai, L. N. He, N. Nakayama, K. Chen, X.M. Sun, X. Y. Chen, H. J. Dai, *Nature Nanotech.*, 47 (2007).
21. J. M. Harris, R. B. Chess, *Nature Rev. Drug Disc.*, 214 (2003).
22. M. A. Willard, L. K. Kurihara, E. E. Carpenter, S. Calvin, V. G. Harris, *Int. Mater. Rev.*, 125 (2004).
23. A. H. Lu, E. L. Salabas, F. Schuth, *Angew. Chemie. Int. Ed.* 1222 (2007).
24. R. Massart, *IEEE Trans. Magn.*, 1247 (1981).
25. T. Sugimoto, E. Matijević, *J. Colloid Interface Sci.,* 227 (1980).
26. L. Babes, B. Denizot, G. Tanguy, J. J. Le Jeune, P. Jallet, *J. Colloid Interface Sci.,* 474 (1999).
27. O. Karaagac, H. Kockar, J. *Supercond. Nov. Magn.*, 2777 (2012).
28. C. Pereira, A. M. Pereira, C. Fernandes, M. Rocha, R. Mendes, M. Paz Fernandez-Garcia, A. Guedes, P. B. Tavares, J. M. Greneche, J. P. raujo, C. Freire, *Chem. Mater.*, 1496 (2012).
29. S. Si, A. Kotal, T. K. Mandal, S. Giri, H. Nakamura, T. Kohara, *Chem. Mater.,* 3489 (2004).
30. S. R. Wan, J. S. Huang, H. S. Yan, K. L. Liu, J. *Mater. Chem.*, 298 (2006).
31. J. H. Lee, Y. M. Huh, Y. Jun, J. Seo, J. Jang, H. T. Song, S. Kim, E. J. Cho, H. G. Yoon, J. S. Suh, J. Cheon, *Nat. Med.*, 95 (2007).
32. S. H. Sun, H. Zeng, *J. Am. Chem. Soc.,* 8204 (2002).
33. T. Hyeon, S. S. Lee, J. Park, Y. Chung, H. B. Na, *J. Am. Chem. Soc.,* 12798 (2001).
34. J. Park, K. An, Y. Hwang, J. G. Park, H. J. Noh, J. Y. Kim, J. H. Park, N. M. Hwang, T. Hyeon, *Nat. Mater.,* 891 (2004).
35. N. R. Jana, Y. Chen, X. Peng, *Chem. Mater*, 3931 (2004).

36. Z. Li, Q. Sun, M. Gao, *Angew. Chem. Int Ed.,* 123 (2005).
37. F. Q. Hu, L. Wei, Z. Zhou, Y. L. Ran, Z. Li, M. Y. Gao, *Adv. Mater.,* 2553 (2006).
38. J. Vidal-Vidal, J. Rivas, M. A. Lo´pez-Quintela, *Colloid. Surf.,* A 44 (2006).
39. C. Okoli, M. Boutonnet, L. Mariey, S. Järås, G. K. Rajarao, *J. Chem. Technol. Biotechnol.* 1386 (2011).
40. M. Darbandi, F. Stromberg, J. Landers, N. Reckers, B. Sanyai, W. Keune, H. Wende, *J. Phys. D*: *Appl. Phys.,* 195001 (2012).
41. F. A. Tourinho, R. Franck, R. Massart, *J. Mater. Sci.,* 3249 (1990).
42. A. B. Chin, I. I. Yaacob, *J. Mater. Process. Technol.* 235 (2007).
43. X. Hu, J. C. Yu, J. Gong, *J. Phys. Chem. C,* 11180 (2007).
44. S. Giria, S. Samantab, S. Majic, S. Gangulic, A. Bhaumikb, *J. Magn. Magn. Mater.* 296 (2005).
45. X. Liu, G. Qiu, A. Yan, Z. Wang, X. Li, J. *Alloy Compd.*, 216 (2007).
46. J. Wang, J. Sun, Q. Sun, Q. Chen, *Mater. Res. Bull.*, 1113 (2003).
47. Y. Zheng, Y. Cheng, F. Bao, Y. Wang, *Mater. Res. Bull.*, 525 (2006).
48. S. Ge, X. Shi, K. Sun, C. Li, J. R. Baker, M. M. Banaszak Holl, B. G. Orr, *J. Phys. Chem. C,* 13593 (2009).
49. J. H. Bang, K. S. Suslick, *J. Am. Chem. Soc.*, 2242 (2007).
50. K. S. Suslick, *Sci.*, 1439 (1990).
51. R. Vijayakumar, Y. Koltypin, I. Felner, A. Gedanken, *Mater. Sci. Eng.*, 101 (2000).
52. J. Pinkas, V. Reichlova, R. Zboril, Z. Moravec, P. Bezdicka, J. Matejkova, *Ultrason. Sonochem.,* 257 (2008)
53. R. J. Joseyphus, D. Kodama, T. Matsumoto, Y. Sato, B. Jeyadevan, K. Tohji, *J. Magn. Magn. Mater.,* 2393 (2007).
54. B. Zhang, Z. Tu, F. Zhao, J. Wang, *Appl. Surface Sci.*, 375 (2013).
55. J.-L. Bridot, D. Stanicki, S. Laurent, S. Boutry, Y. Gossuin, P. Leclère, R. Lazzaroni, L. Vander Elst, R. N. Muller, *Contrast Med. Mol. Imaging*, 466 (2013).
56. D. Forge, A. Roch, S. Laurent, H. Tellez, Y. Gossuin, F. Renaux, L. Vander Elst, R. N. Muller. *J. Phys. Chem. C*, 19178 (2008).
57. A. G. Roca, R. Costo, A. F. Rebolledo, S. Veintemillas-Verdaguer, P. Tartaj, T. Gonzalez-Carreno, M. P. Morales, C. J. Sema, *J. Phys. D*: *Appl. Phys.*, 224002 (2009).

58. H. Lee, M. K. Yu, S. Park, S. Moon, J. J. Min, Y. Y. Jeong, H. W. Kang, S. Jon, *J. Am. Chem. Soc.*, 12739 (2007).
59. R. De Palma, S. Peeters, M. J. Van Bael, H. Van den Rul, K. Bonroy, W. Laureyn, J. Mullens, G. Borghs, G. Maes, *Chem. Mater.*, 1821 (2007).
60. N. Kohler, G. E. Fryxell, M. Zhang, *J. Am. Chem. Soc.*, 7206 (2004).
61. E. K. U. Larsen, T. Nielsen, T. Wittenborn, H. Birkedal, T. Vorup-Jensen, M. H. Jakobsen, L. Ostergaard, M. R. Horsman, F. Besenbacher, K. A. Howard, J. Kjems, *ACS Nano*, 1947 (2009).
62. T. Ninjbadgar, D. F. Brougham, *Adv. Funct. Mater.*, 4769 (2011).
63. E. E. Carpenter, C. Sangregorio, C. J. O'Connor, *IEEE Trans. Magn.,* 3496 (1999).
64. H. Maleki, A. Simchi, M. Imani, B. F. O. Costa, *J. Magn. Magn. Mater.,* 3997 (2012).
65. L. Maurizi, H. Bisht, F. Bouyer, N. Millot, *Langmuir*, 8857 (2009).
66. N. Miguel-Sancho, O. Bomatí-Miguel, G. Colom, J. P. Salvador, M. P. Marco, *Chem. Mater.*, 2795 (2011).
67. H. Benbenishty-Shamir, R. Gilert, I. Gotman, E. Y. Gutmanas, C. N. Sukenik, *Langmuir,* 12082 (2011).
68. T. J. Daou, J. M. Greneche, G. Pourroy, S. Buathong, A. Derory, C. Ulhaq-Bouillet, B. Donnio, D. Guillon, S. Begin-Colin, *Chem. Mater.*, 5869 (2008).
69. A. Karimi, B. Denizot, C. Passirani, F. Hindré, J. Roux, P. Legras, J. J. Lejeune, *Eur. J. Pharm. Sci.*, 101 (2013).
70. Y. Lalatonne, C. Paris, J. M. Serfaty, P. Weinmann, M. Lecouvey, L. Motte, *Chem. Commun.*, 2553 (2008).
71. J. A. Park, J. J. Lee, I. S. Kim, B. H. Park, G. H. Lee, T. J. Kim, H. C. Ri, H. J. Kim, Y. Chang, *Colloids Surf. A*, 288 (2008).
72. Q. Quan, J. Xie, H. Gao, M. Yang, F. Zhang, G. Liu, X. Lin, A. Wang, H. S. Eden, S. Lee, G. Zhang, X. Chen, *Mol. Pharm.*, 1669 (2011).
73. J. Xie, J. Wang, G. Niu, J. Huang, K. Chen, X. Li, X. Chen, *Chem. Commun.*, 433 (2010).
74. C. Boyer, M. R. Whittaker, V. Bulmus, J. Liu, T. P. Davis, *NPG Asia Materials*, 23 (2010).
75. D. Forge, A. Roch, S. Laurent, H. Tellez, Y. Gossuin, L. Vander Elst, R. N. Muller, *J. Phys. Chem. C*, 19178 (2008).

76. A. M. G. C. Dias, A. Hussain, A. S. Marcos, A. C. A. Roque, *Biotechnology Advances*, 142 (2011).
77. M. Chanana, Z. Mao, D. Wang, *J. Biomed. Nanotechnol.*, 652 (2009).
78. L. Yun Tack, W. Kyoungja, C. Kyu-Sil, *IEEE Transactions Nanotechnol.*, 111 (2008).
79. M. C. Bautista, O. Bomati-Miguel, M. del Puerto Morales, C. J. Serna, S. Veintemillas-Verdaguer, *J. Magn. Magn. Mater.*, 20 (2005).
80. S. L. Easo, P. V. Mohanan, *Carbohyd. Polym.*, 726 (2013).
81. J. E. Rosen, L. Chan, D. B. Shieh, F. X. Gu, *Nanomedicine*: *NBM*, 275 (2012).
82. L. Josephson, C. H. Tung, A. Moore, R. Weissleder, *Bioconjug. Chem.,* 186 (1999).
83. J. R. McCarthy, R. Weissleder, *Adv. Drug Del. Rev.,* 1241 (2008).
84. J. Deng, J. He, J. S. Zheng, S. Terakawa, H. Huang, L. C. Fang, Y. Li, P. Cheng, L. L. Jiang, *Particul. Sci. Tech.*, 241 (2012).
85. E. Duguet, S. Vasseur, S. Mornet, G. Goglio, A. Demourgues, J. Portier, F. Grsset, P. Veverka, E. Pollert, *Bull. Mater. Sci.,* 581 (2006).
86. S. Chaleawlert-Umpon, V. Mayen, K. Manotham, N. Pimpha, *J. Biomater. Sci.,* 1515 (2010).
87. A. Szpak, G. Kania, T. Skórka, W. Tokarz, S. Zapotoczny, M. Nowakowska, *J. Nanopart. Res.,* 1 (2012).
88. Z. T. Tsai, J. F. Wang, H. Y. Kuo, C. R. Shen, J. J. Wang, T. C. Yen, *J. Magn. Magn. Mater.,* 208 (2010).
89. B. Gaihre, M. S. Khil, D. R. Lee, H. Y. Kim, *Int. J. Pharm.*, 180 (2009).
90. M. L. Ma, X. R. Qi, Y. Maitani, T. Nagai, *Int. J. Pharm.*, 177 (2007).
91. F. Gao, Y. Cai, J. Zhou, X. Xie, W. Ouyang, Y. Zhang, X. Wang, X. Zhang, X. Wang, L. Zhao, J. Tang, *Nano Res.*, 23 (2010).
92. F. Y. Cheng, S. P. Wang, C. H. Su, T .L. Tsai, P. C. Wu, D. B. Shieh, J. H. Chen, P. C. Hsieh, C. S. Yeh, *Biomaterials,* 2104 (2008).
93. S.-J. Lee, J.-R. Jeong, S.-C. Shin, J.-C., Kim, Y.-H. Chang, Y.-M. Chang, J.-D. Kim, *J. Magn. Magn. Mater.*, 2432 (2004).
94. L. Zhou, B. He, F. Zhang, *ACS Appl. Mater. Inter.*, 192 (2011).
95. A. Garcia, A. Tercjak, N. E. Zafeiropoulos, M. Stamm, I. Mondragon, *J. Polymer Sci. Part A*: *Polym. Chem.,* 4744 (2007).

96. S.-J. Bae, J.-A. Park, J.-J. Lee, G.-H. Lee, T.-J. Kim, D.-S. Yoo, Y. Chang, *Curr. Appl. Phys.*, 19 (2009).
97. Y. Y. Xu, M. Zhou, H. J. Geng, J. J. Hao, Q. Q. Ou, S. D. Qi, H. I. Chen, X. G. Chen, *Appl. Sur. Sci.*, 3897 (2012).
98. A. Masotti, A. Pitta, G. Ortaggi, M. Corti, C. Innocenti, A. Lascialfari, *Magn. Reson. Mater. Phys., Bio., Med.*, 77 (2009).
99. S. C. McBain, U. Griesenbach, S. Xenariou, A. Keramane, C. D. Batich, E. Alton, J. Dobson, *Nanotechnol.*, 19 (2008).
100. I. K. Park, C. P. Ng, J. Wang, B. Chu, C. Yuan, S. Zhang, S. H. Pun, *Biomaterials*, 724 (2008).
101. Y. Ge, S. Zhang, S. He, Y. Zhang, N. Gu, *J. Nanosci. Nanotechnol*, 1287 (2009).
102. K. Herve, L. Douziech-Eyrolles, E. Munnier, S. Cohen-Jonathan, M. Souce, H. Marchais, P. Limelette, F. Warmont, M. L. Saboungi, P. Dubois, I. Chourpa, *Nanotechnol.*, 19 (2008).
103. J. Y. Park, P. Daksha, G. H. Lee, S. Woo, Y. M. Chang, *Nanotechnol.*, 19 (2008).
104. T. Shen, R. Weissleder, M. Papisov, A. Bogdanov, T. J. Brady, *Magn. Reson. Med.*, 599 (1993).
105. V. Plassat, M. S. Martina, G. Barratt, C. Menager, S. Lesieur, *Int. J. Pharm.*, 118 (2007).
106. Y. Bae, T. A. Diezi, A. Zhao, G. S. Kwon, *J. Control Release*, 324 (2007).
107. J. Gang, S. -B. Park, W. Hyung, E. H. Choi, J. Wen, H. -S. Kim, Y. -G. Shul, S. Haam, S. Young Song, *J Drug Target*, 445 (2007).
108. J. H. Lee, Y. M. Huh, Y. W. Jun, J. W. Seo, J. T. Janq, H. T. Song, S. Kim, E. J. Cho, H. G. Yoon, J. S. Suh, J. Cheon, *Nat. Med.*, 95 (2007).
109. A. L. Glover, J. B. Bennett, J. S. Pritchett, S. M. Nikles, D. E. Nikles, J. A. Nikles, C. S. Brazel, *IEEE Trans. Magn.*, 231 (2013).
110. M. Talelli, C. J. F. Rijcken, T. Lammers, P. R. Seevinck, G. Storm, C. F. van Nostrum, W. E. Hennink, *Langmuir*, 2060 (2009).
111. W. T. Al-Jamal, K. Kostarelos, *Nanomed.* 85 (2007).
112. H. De Oliveira, J. Thevenot, S. Lecommandoux, *Nanomed. Nanobiotechnol.*, 525 (2012).

113. Z. Y. Qiao, R. Ji, X. N. Huang, F. S. Du, R. Zhang, D. H. Liang, Z. C. Li, *Biomacromol.*, 1555 (2013).
114. B. Chertok, B. A. Moffat, A. E. David, F. Yu, C. Bergemann, B. D. Ross, V. C. Yang, *Biomater.*, 487 (2008).
115. L. Yang, Z. Cao, H. K. Sajja, H. Mao, L. Wang, H. Huaying, H. Xu, T. Jiang, W. C. Wood, S. Nie, Y. A. Wang, *J. Biomed. Nanotechnol.*, 439 (2008).
116. Y. Chang, X. Meng, Y. Zhao, K. Li, B. Zhao, M. Zhu, Y. Li, X. Chen, J. Wang, *J. Colloid Interface Sci.*, 403 (2011).
117. S. H. Wang, X. Shi, M. Van Antwerp, Z. Cao, S. D. Swanson, X. Bi, J. R. Baker, *Adv. Funct. Mater.*, 3043 (2007).
118. J. K. Oh, J. M. Park, *Progr. Polymer Sci.*, 168 (2011).
119. G. M. Lanza, P. Winter, S. Caruthers, A. Schmeider, K. Crowder, A. Morawski, H. Zhang, M. J. Schott, S. A. Wickline, *Curr. Pharm. Biotechnol.*, 495 (2004).
120. M. Atri, *J. Clin. Oncol.*, 3299 (2006).
121. X. Yang, J. J. Grailer, I. J. Rowland, A. Javadi, S. A. Hurley, V. Z. Matson, D. A. Steeber, S. Gong, *ACS Nano*, 6805 (2010).
122. M. Kumar, M. Yigit, G. Dai, A. Moore, Z. Medarova, *Cancer Res.*, 7553 (2010).
123. J. Yang, C.-H. Lee, H. J. Ko, J.-S. Suh, H.-G. Yoon, K. Lee, Y.-M. Huh, S. Haam, *Angew. Chem. Int. Ed.* 46, 8836–8839 (2007).
124. M. Liong, J. Lu, M. Kovochich, T. Xia, S. G. Ruehm, A. E. Nel, F. Tamanoi, J. I. Zink, *ACS Nano* 889 (2008).
125. S. S. Kelkar, T. M. Reineke, *Bioconjug. Chem.*, 1879 (2011).
126. B. T. Luk, L. Zhang, *ACS Appl. Mater. Interfaces*, under press, 6, 21859 (2014).
127. S. Svenson, *Mol. Pharmaceutics*, 848 (2013).
128. F. Danhier, A. Le Breton, V. Préat, *Mol. Pharmaceutics*, 2961 (2012).